Chaos, Solitons and Fractals 143 (2021) 110549

Contents lists available at ScienceDirect

Chaos, Solitons and Fractals

Nonlinear Science, and Nonequilibrium and Complex Phenomena

journal homepage: www.elsevier.com/locate/chaos

On the organic memristive device resistive switching efficacy☆

Yuriy Gerasimov[a,b,*], Evgenii Zykov[a,b], Nikita Prudnikov[d], Max Talanov[a,b], Alexander Toschev[a], Victor Erokhin[c,d,e]

[a] Neuromorphic Computing and Neurosimulations Laboratory at Kazan Federal University, Russia
[b] Neuroscience Laboratory at Kazan Federal University, Russia
[c] Electronic Synapse Laboratory at Kazan Federal University, Russia
[d] National Research Centre Kurchatov Institute, Russia
[e] Consiglio Nazionale delle Ricerche at Istituto dei Materiali per l'Elettronica ed il Magnetismo, Italy

ARTICLE INFO

Article history:
Received 11 August 2020
Revised 16 November 2020
Accepted 4 December 2020

Keywords:
Memristive device
Organic memristors
Neuromorphic computing
Electronics
Engineering

ABSTRACT

This paper is dedicated to the experimental study of learning properties of systems, based on polyaniline (PANI) memristive devices. Signals with different forms, amplitudes, frequencies have been used as external stimuli and it has been demonstrated their different influence over memristive device conductance. According to the obtained results, pulse width modulation seems the most adequate method for the implementation of neuromorphic circuits.

1. Introduction

During recent 12 years memristive devices [1,2] attract significant attention, as analogues of biological synapses in electronic circuits [3–5]. We see a lot of applications and implementations including STDP [6–11], memristor crossbars [12] and different types of neural networks [13–16].

Recently the progress in memeristive devices indicated the milestone when it has been demonstrated the prototype of the synaptic prosthesis [17] that effectively connects two not connected naturally neurons in the slice of rat neocortex.

There are different materials used to realise memristive devices[18–20]. The working principle of the most of them is based on the growth of conducting filaments in thin insulating films between metal oxide layers with successive variation of their conductance [21,22]. This mechanism is rather random and could not be well controlled, that leads to the uncertainty of voltage values, required for switching in *ON* and *OFF* conductivity state, not only from one device to the other, but also within different cycles of the same device [23]. This fact makes it difficult to use these devices for neuromorphic applications and it is the main reason why the additional circuitry is usually required to work with these uncertainties. However, rather gradual resistance switching has been observed recently in similar systems [24].

Conductivity switching is intrinsically noisy phenomenon in such kinds of devices [25,26]. Similarly to well-known effects in complex systems [27–30], noise can play a positive role also in memristive devices [31–33].

With that in mind, it has been proposed that polyaniline based memristive devices can become a perspective alternative, since *ON* and *OFF* voltages are fixed and depend only on the device architecture [34,35].

Up to now there is only one paper, dedicated to the noise effect on this type of memristive device [36]. It has been demonstrated that external noise plays a positive role also in this case.

The working principle of this device is based on the significant difference of polyaniline conductivity in its reduced and oxidized states. Redox reactions occur in the active zone of contact of polyaniline with solid electrolyte (polyethylene oxide + LiClO4). Variation of the electronic conductivity in polyaniline channel is due to the ion motion between the conducting polymer and solid electrolyte as it was directly shown spectroscopic methods [37] and X-ray fluorescence [38], and described by the developed models [39,40].

☆ The reported study was funded by RFBR according to the research project N19-29-03057. The part of this work is performed according to the Russian Government Program of Competitive Growth of Kazan Federal University.

* Corresponding author at: Neuromorphic Computing and Neurosimulations Laboratory at Kazan Federal University, Russia.

E-mail addresses: yurger2009@gmail.com (Y. Gerasimov), Evgeniy.Zykov@kpfu.ru (E. Zykov), nikprud321@gmail.com (N. Prudnikov), max.talanov@gmail.com (M. Talanov), sanchis.no@gmail.com (A. Toschev), victor.erokhin@imem.cnr.it (V. Erokhin).

https://doi.org/10.1016/j.chaos.2020.110549
0960-0779/

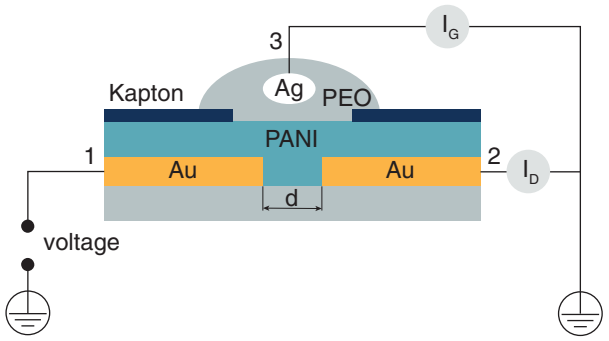

Fig. 1. Schematic of the internal structure of the organic memristive device and test setup connection 1 and 2 connected to gold electrodes, 3 connected to silver wire.

The first successful demonstration of the use of these devices as a synapse consisted of reconstruction of a part of nervous system of the pond snail Lymnaea stagnalis responsible for learning during feeding [41]. It is to note, that the implemented circuit not only imitated the association of initially neutral stimulus with the presence of food, but also reconstructed the architecture of the part of nervous system, where memristive devices were directly integrated in the position of synapses.

Three recently published papers underline other important properties required for parts of nervous system prosthesis. In particular, they demonstrate the importance of the temporal correlation of pre- and post-synaptic spikes on the conductivity state of the memristive device. First, it has been demonstrated that the strength of the memristive connections depends not only on the number of passed pulses but also on the their frequency[42]. Second paper shows, that STDP (spike timing dependent plasticity) learning mechanism can be implemented in circuits, based on organic memristive devices [43,44]. Finally, the organic memristive device was used as synaptic connection between two nervous cells from the rat neocortex [17] using natural spiking of neurons.

The possible utilisation of memristive devices as a key model elements of circuits, mimicking biological neurons, was studied and electronic circuit prototypes were proposed [45–47]. To make further improvements, we consider that it is necessary to study the influence of different training signals types, in order to make the most efficient use of the memristive devices in our schemes.

In this work we tried to identify roles of external stimuli on the resistive switching capabilities of organic memristive devices.

2. Materials and methods

The internal structure of the memeristive device is presented in Fig. 1 [48]. The technology of the memristive device production is as following: polyaniline (PANI in Fig. 1, Mw=10^5 Da, Sigma-Aldrich) is dissolved in

N-methylpirrolidome (NMP) with a concentration of 3 g/L and then diluted with 9:1 NMP/Toluene mixture to receive the solution with a concentration of 0.3 g/L. Polyethylene oxide (PEO in Fig. 1, Mw $= 6 * 10^5$ Da. Sigma-Aldrich) is dissolved in the 0.23 mole lithium perchlorate aqueous solution with the concentration of 50 g/L. After that electrolyte solution is diluted with a 1 mol HCl aqueous solution in a ratio of 9:1 (PEO/HCl). The PANI active channel is formed on a silicon oxide substrate with preliminary evaporated and photolithographically patterned gold electrodes (Au in Fig. 1) by the Langmuir-Schaefer technique.

The distance between electrodes that is referenced as d in Fig. 1 is set to 10 μm. 10 PANI layers are consequentially transferred on these substrates. After transferring the PANI films are dried and doped in HCl vapor. The area around the active channel is covered by a Kapton film to avoid redox reactions outside of the channel (Kapton in Fig. 1). Later a drop of PEO electrolyte is placed on the active zone and dried in a airflow, right before the drop is dried completely, we insert the silver wire with a diameter of 50 μm into the drop (Ag in Fig. 1).

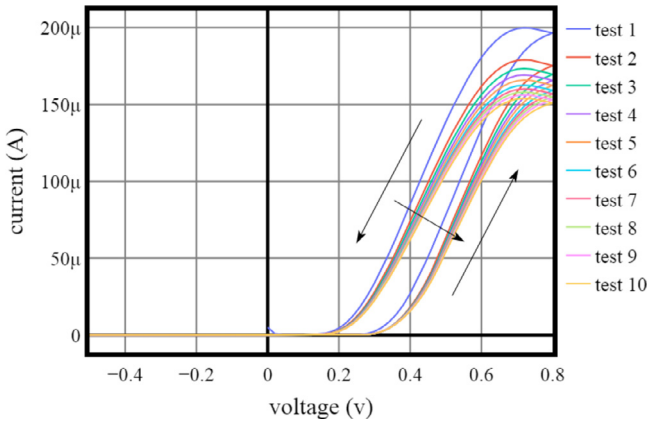

Fig. 2. I-V curves of I_D current of experimental memristive device. Coloured lines indicate the test number that runs the voltage loop from −0.5 to +0.8V.

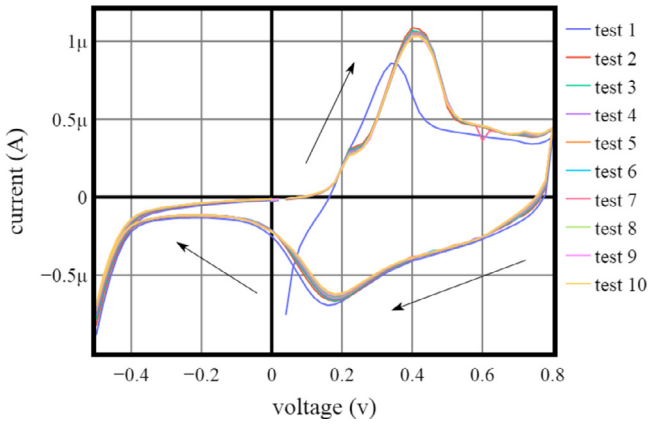

Fig. 3. I-V curves of I_G current of experimental memristive device. Coloured lines indicate the test number that runs the voltage loop from −0.5 to +0.8V.

We used the Keysight B2902A Precision Source/Measure Unit for I-V curve measurement and the AM measurement whereas for the PWM and the FM we use the NI PXIe-4140 Source Measure Unit. In our experiments the input voltage is applied to the gold electrodes (voltage label in Fig. 1) in the range: $-0.5 \ldots +0.8$ V, this range is adequate for the redox reactions in our PANI memristive device, necessary for the resistive switching, but does not cause the irreversible overoxidation processes.

3. Results

3.1. Current-voltage characteristics

In order to understand basic dynamics of the memristive device resistive switching the current-voltage characteristics have been studied (Figs. 2, 3).

The voltage loop we used during experiments was in the range of $-0.5 \ldots +0.8$ V with the step of 0.02 V and duration of each step 0.02 s. We started from 0 V and increased the voltage up to 0.8 V and then reduced down to −0.5 V.

We applied this voltage loop multiple times consequently to check the stability of the I-V characteristics of the device. We measure two currents: going through the device I_D and the ionic current coming through the electrolyte I_G shown in Fig. 1.

Fig. 2 shows typical I–V curves of the current I_D, measured across the device. During the experiment the voltage of the switching from high resistance state to a low one of the device was always stable corresponding to $\sim +0.3$ V (that corresponds to $\sim$ 800 kω with $+0.4$ V and about $5 - 6$ kω with $+0.8$ V). The maximum current value decreased continuously during successive cycles of the applied voltage loop from 200 μA down to 150 μA, and this correlates with previous PANI memristive devices experiments [48].

The I-V curve of the ionic current (I_G) is shown in Fig. 3 and it represents oxidizing (positive maximum) and reduction (negative minimum) potentials of the PANI film with the same trend to decrease during the experiment from loop to loop applied.

3.2. Dynamic characteristics

We tested, different types of the modulation of the input signal of the PANI memristive device such as amplitude modulation (AM), frequency modulation (FM) with defined amplitude, and pulse width modulation (PWM) with defined frequency and amplitude.

We conducted two kinds of experiments (1) the PANI memristive device conductance increasing (potentiation), (2) the conductance decreasing (depression). To reduce the instability of the memristor device characteristics, before each series of experiments, we applied the control additional voltage cycle (Figs. 2, 3) described in the Section 2).

We were not interested in the absolute values of ON and OFF voltages of the memristive device, but only temporal changes of the characteristics of its resistance, indicating the effectiveness of the specific type of modulation. The application of relative parameters (resistance gradient) allowed us to reduce the influence of instability of the characteristics of the memristive device.

Before the AM potentiation experiment, we depressed the device by the voltage of -0.5 V for five minutes whereas before the AM depression, we potentiated the device by the voltage of $+0.7$ V also for five minutes.

We ran PWM and FM experiments in 2-channel mode, the Ag-wire was connected to one of the substrate gold electrodes and it was used to apply lower voltage to the device. The amplitude of PWM and FM signals was set to 0.7 V, the frequency of the PWM signal was set to 100 Hz. To initiate the electrochemical reactions in the PANI memristive device we applied the voltage around 0.4 V, as it is shown in Fig. 2.

We measured the I_D current once per pulse period during the application to the memristive device. Sometimes the measurement of the current was performed not at the moment of a maximal voltage amplitude applied that's why the FM and PWM figures have some random pikes (Figs. 5, 9).

Figs. 4–9 show the typical current through the device as the function of time with different types of applied signals. Figs. 4, 8, 6 show memristive device behaviour during the potentiation and Figs. 7–9 show the behaviour during the depression.

Fig. 4 indicates the gradual increase of the current I_D with different potentiation voltages during the amplitude modulation experiment. The voltage of 0.3 V almost does not affect the PANI memristive device conductance increasing the current to ~ 10 μA during the 40 s. The application of $0.5 \ldots 0.9$ V amplitudes affect the device in much more intensive dynamical way increasing the current I_D up to 110,150 and 190 μA respectively. It is to note, that the saturation current for the applied 0.9 V is less than for 0.7 V. It is due to the fact, that a positive voltage, applied to the device for a rather long time, should not be higher than 0.7 V, because it can result in the irreversible overoxidation of polyaniline, that has higher resistance value [35].

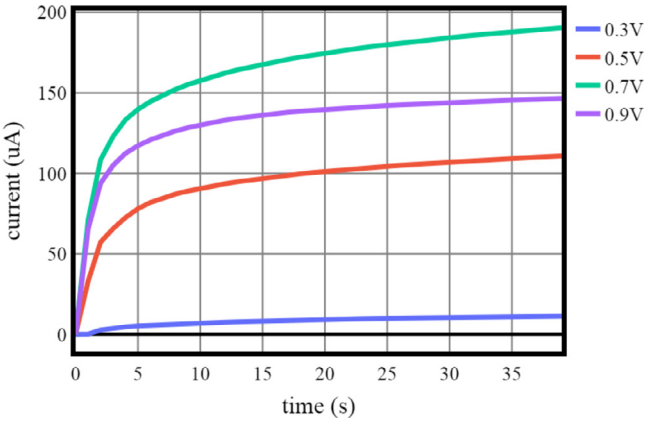

Fig. 4. I_D current change over time during AM potentiation. The blue line stands for 0.3V, the red line stands for 0.5V, the green line – 0.7V, the lilac line – 0.9V. (For interpretation of the references to colour in this figure legend, the reader is referred to the web version of this article.)

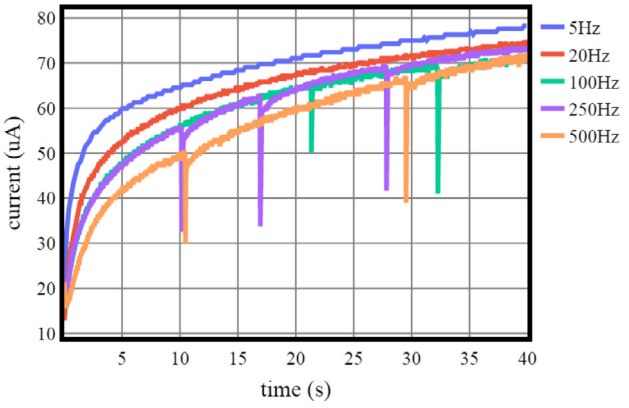

Fig. 5. I_D current change over time during FM potentiation The blue line stands for 5Hz, the red line stands for 20Hz, the green line – 100Hz, the lilac line – 250Hz, the orange line – 500Hz. (For interpretation of the references to colour in this figure legend, the reader is referred to the web version of this article.)

The results of the frequency modulated signal experiments are presented in Fig. 5. Changing the frequency we observed less significant influence over resistance switch than in case of AM effect over the I_D current. With 5 Hz the I_D increased to almost 80 μA within 40 s. It is interesting, that increasing frequency leads to decreasing maximum current value within 40 s period. We suppose that the possible reason for this is that ions can not manage to transfer between PEO and PANI layers of the memeristive device during the short period of time.

In Fig. 6 the PWM signal with low duty cycle 20% has no effect on conductance of the memeristive device, while input signals with 40% duty cycle reach almost 40 μA during 40 s, signals with 60% duty cycle reach almost 120 μA within 40 s and has similar to 0.5 V of the AM potentiation behaviour (Fig. 4), and 80% duty cycle signals comes close to the 0.7 V of the AM potentiation, getting slightly above 180 μA during 40 s.

Fig. 7 represents the results of the depression of the memristive device conductivity during the amplitude modulation. All applied voltages show almost similar effect, decreasing conductance to minimal values during the same period of about 8 s. It is interesting that even low positive voltage can lead the memristive device conductance to decrease (the reduction potential is about $+0.1$ V). We suppose that all the PANI memristive devices should use the constant resting voltage on memristive device, in order to keep resistance from decline. The presence of the positive current in the case of applied negative voltage is due to the transition pro-

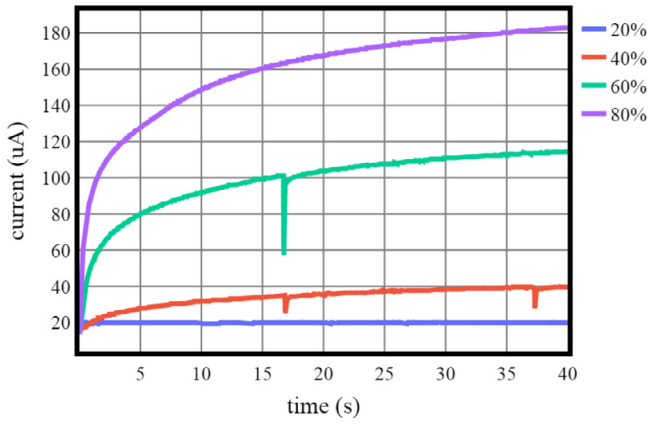

Fig. 6. I_D current change over time during PWM potentiation. The blue line stands for 20% of the duty cycle, the red line stands for 40%, the green line – 60%, the lilac line – 80%. (For interpretation of the references to colour in this figure legend, the reader is referred to the web version of this article.)

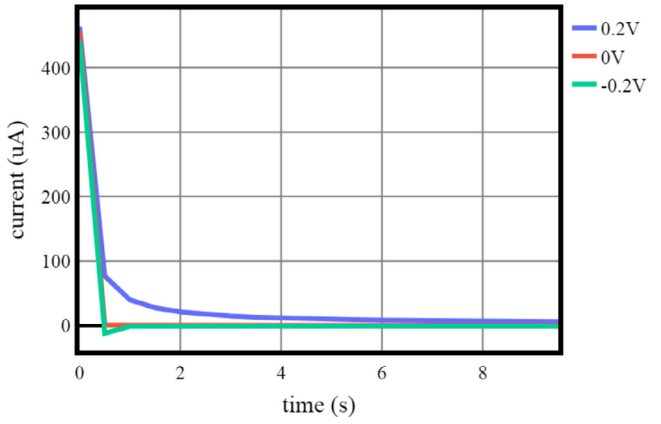

Fig. 7. I_D current change over time during AM depression. The blue line stands for +0.2V, the red line stands for 0.0V, the green line stands for −0.2V. (For interpretation of the references to colour in this figure legend, the reader is referred to the web version of this article.)

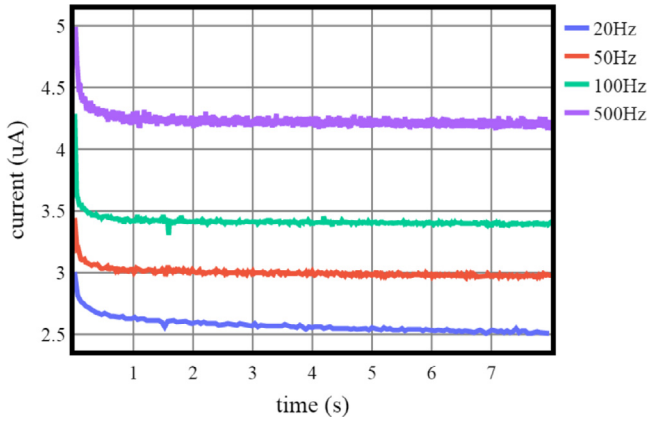

Fig. 8. I_D current change over time during FM depression. The blue line stands for 20Hz, the red line stands for 50Hz, the green line – 100Hz, the lilac line – 500Hz. (For interpretation of the references to colour in this figure legend, the reader is referred to the web version of this article.)

cesses, connected to the discharge of the capacitor, existing at the interface between polyaniline and polyethylene oxide.

The FM depression shown in Fig. 8 indicates that lower frequencies provide higher impact over the memristive device conductivity. For example the 500 Hz signal decreases I_D to nearly

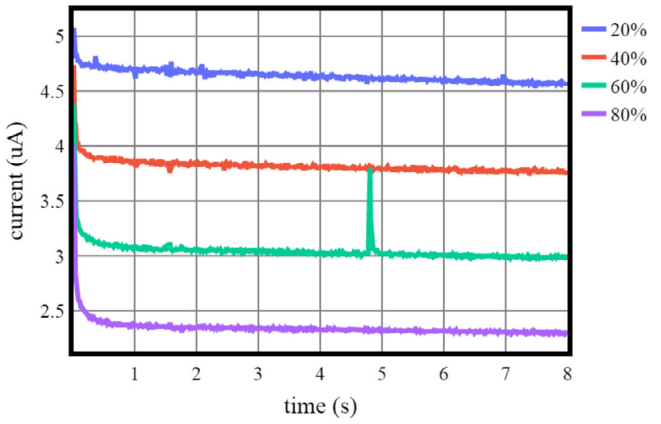

Fig. 9. I_D current change over time during PWM depression. The blue line stands for 20% of the duty cycle, the red line stands for 40%, the green line – 60%, the lilac line – 80%. (For interpretation of the references to colour in this figure legend, the reader is referred to the web version of this article.)

4 μA per 8 s, whereas 20 Hz decreases the current to 2.5 μA within same time.

PWM depression shown in Fig. 9, as well shows the consequent decrease of the conductance with duty cycle increase. Starting at almost no impact at 20% and coming close to −0.2 V AM dynamics at 80%.

4. Discussion

We suppose that it is very important to analyse kinetics of the conductivity variation due to different applied stimuli to memristive devices for the majority of neuromorphic applications. Here we presented the results, of amplitude, frequency and pulse width modulations applied to inputs signals.

In the case of AM experiments, we observed a gradual increase of the output current amplitude and the speed of resistive switching with the increase of the applied voltage. Switching to the *OFF* state was always faster and its kinetics was more or less constant.

In the case of FM experiments, we observed the increase of current and the decrease of the resistive switching speed, which is correlated to the redox reactions, involving ion exchange between PANI and PEO layers (ion mobility in the solid phase is rather low). Considering the amplitude of the output current, it seems similar for all frequencies in the saturation region.

It is to note, that AM and PWM experiments results indicate very similar kinetics: 190 μA during 40 s. The PWM potentiation shows 180 μA during 40 s at 80% duty cycle, keeping in mind, that 100% duty cycle will be same as 0.7 V AM.

As for depression, we indicate that differences in current values are not so high, and main conductance reduction happens within 8 . . . 10 s, that is faster, than for potentiation (that usually takes place during whole experiment 40 s). Since AM and PWM experiments results shows similar curves, the PWM seems more adequate to use for neuromorphic applications, because it corresponds better to the biological benchmarks, where the amplitude of spikes is more or less stable, but the frequency and inter spike intervals are useful for the potentiation and depression of synaptic strength in STDP approach.

5. Conclusion

We conducted series of experiments to identify most usefull and effective way to manage the PANI memristive device resistance using three modes: AM, FM and PWM for both potentiation and depression.

The results of the PANI memristive device potentiation experiments indicated that the highest speed of the resistive switching was in the case of the AM potentiation with the amplitude of 0.7 V during 40 s, the value of the I_D current reached almost the 200 μA. Close to the AM kinetics was demonstrated by pulse width modulation with 180 μA reached during 40 s.

For the depression case we indicate similar close speeds of resistive switching with insignificant variations in all three cases of AM, FM and PWM.

This way we could indicate that most useful way to manage the PANI memristive device resistance is PWM with duty cycle 80%.

Declaration of Competing Interest

The authors declare that they have no known competing financial interests or personal relationships that could have appeared to influence the work reported in this paper.

CRediT authorship contribution statement

Yuriy Gerasimov: Conceptualization. **Evgenii Zykov:** Conceptualization. **Nikita Prudnikov:** Writing - original draft, Writing - review & editing. **Max Talanov:** Conceptualization. **Alexander Toschev:** Writing - original draft, Methodology. **Victor Erokhin:** Writing - original draft, Methodology.

Acknowledgements

The work partly is performed according to the Russian Government Program of Competitive Growth of Kazan Federal University. The reported study was partly funded by RFBR according to the research project N19-29-03057 Memristive elements based on polyconjugated organic semiconductor functional materials for the implementation of model bio-plausible neuromorphic networks.

References

[1] Chua M. Memristor - the missing circuit element. IEEE Trans Circuit Theory 1971;18:507–19.
[2] Strukov D, Snider D, Stewart D, Williams R. The missing memristor found. Nature 2008;453:80–3.
[3] Jo S, Chang T, Ebong I, Bhadviya B, Mazumder P, Lu W. Nanoscale memristor device as synapse in neuromorphic systems. Nano Lett 2010;10:1297–301.
[4] Wang Z, Joshi S, Savel'ev S, Jiang H, Midya R, Lin P, et al. Memristors with diffusive dynamics as synaptic emulators for neuromorphic computing. Nat Mater 2017;16:101–8.
[5] del Valle J, Ramírez JG, Rozenberg MJ, Schuller IK. Challenges in materials and devices for resistive-switching-based neuromorphic computing. Journal of Applied Physics 2018;124(21):211101. doi:10.1063/1.5047800. http://aip.scitation.org/doi/10.1063/1.5047800.
[6] Lu K, Li Y, He W-F, Chen J, Zhou Y-X, Duan N, et al. Diverse spike-timing-dependent plasticity based on multilevel HfO x memristor for neuromorphic computing. Applied Physics A 2018;124(6):438. doi:10.1007/s00339-018-1847-3. http://link.springer.com/10.1007/s00339-018-1847-3.
[7] Yang R, Huang H-M, Hong Q-H, Yin X-B, Tan Z-H, Shi T, et al. Synaptic suppression triplet-STDP learning rule realized in second-order memristors. Adv Funct Mater 2018;28(5):1704455. doi:10.1002/adfm.201704455.
[8] Kim S, Du C, Sheridan P, Ma W, Choi S, Lu WD. Experimental Demonstration of a Second-Order Memristor and Its Ability to Biorealistically Implement Synaptic Plasticity. Nano Letters 2015;15(3):2203–11. doi:10.1021/acs.nanolett.5b00697. https://pubs.acs.org/doi/10.1021/acs.nanolett.5b00697.
[9] Linares-Barranco B, Serrano-Gotarredona T, Camuñas-Mesa LA, Perez-Carrasco JA, Zamarreño-Ramos C, Masquelier T. On spike-timing-dependent-plasticity, memristive devices, and building a self-learning visual cortex. Front Neurosci 2011;5:26.
[10] Wang ZQ, Xu HY, Li XH, Yu H, Liu YC, Zhu XJ. Synaptic learning and memory functions achieved using oxygen ion migration/diffusion in an amorphous ingazno memristor. Adv Funct Mater 2012;22(13):2759–65.
[11] Serrano-Gotarredona T, Masquelier T, Prodromakis T, Indiveri G, Linares-Barranco B. STDP and STDP variations with memristors for spiking neuromorphic learning systems. Front Neurosci 2013;7:2.
[12] Pi S, Li C, Jiang H, Xia W, Xin H, Yang JJ, et al. Memristor crossbar arrays with 6-nm half-pitch and 2-nm critical dimension. Nat Nanotechnol 2019;14(1):35–9. doi:10.1038/s41565-018-0302-0.
[13] Li C, Belkin D, Li Y, Yan P, Hu M, Ge N, et al. Efficient and self-adaptive in-situ learning in multilayer memristor neural networks. Nature Communications 2018;9(1):2385. doi:10.1038/s41467-018-04484-2. http://www.nature.com/articles/s41467-018-04484-2.
[14] Bayat FM, Prezioso M, Chakrabarti B, Nili H, Kataeva I, Strukov D. Implementation of multilayer perceptron network with highly uniform passive memristive crossbar circuits. Nature Communications 2018;9(1):2331. doi:10.1038/s41467-018-04482-4. http://www.nature.com/articles/s41467-018-04482-4.
[15] Wang Z, Joshi S, Savel'ev S, Song W, Midya R, Li Y, et al. Fully memristive neural networks for pattern classification with unsupervised learning. Nature Electronics 2018;1(2):137–45. doi:10.1038/s41928-018-0023-2. http://www.nature.com/articles/s41928-018-0023-2.
[16] Pershin Y, Ventra M. Experimental demonstration of associative memory with memristive neural networks. Neural Netw 2010;23:881–6.
[17] Juzekaeva E, Nasretdinov A, Battistoni S, Berzina T, Iannotta S, Khazipov R, et al. Coupling cortical neurons through electronic memristive synapse. Adv Mater Technol 2019;4:1800350.
[18] Wang Z, Wu H, Burr GW, Hwang CS, Wang KL, Xia Q, et al. Resistive switching materials for information processing. Nature Reviews Materials 2020;5(3):173–95. doi:10.1038/s41578-019-0159-3. http://www.nature.com/articles/s41578-019-0159-3.
[19] Mehonic A, Shluger AL, Gao D, Valov I, Miranda E, Ielmini D, et al. Silicon Oxide (SiO_x): A Promising Material for Resistance Switching? Advanced Materials 2018;30(43):1801187. doi:10.1002/adma.201801187.
[20] Wang M, Cai S, Pan C, Wang C, Lian X, Zhuo Y, et al. Robust memristors based on layered two-dimensional materials. Nature Electronics 2018;1(2):130–6. doi:10.1038/s41928-018-0021-4. http://www.nature.com/articles/s41928-018-0021-4.
[21] Valov I, Linn E, Tappertzhofen S, Schmelzer S, van den Hurk J, Lentz F, et al. Nanobatteries in redox-based resistive switches require extension of memristor theory. Nat Commun 2013;4:1771.
[22] A Younis A, Chu D, Li S. Evidence of filamentary switching in oxide-based memory devices via weak programming and retention failure analysis. Sci Rep 2015;5:13599.
[23] AN Mikhailov A, Belov A, Guseinov D, Korolev D, Antonov I, Efimovykh D, et al. Bipolar resistive switching and charge transport in silicon oxide memristor. Mater Sci Eng B 2015;194:48–54.
[24] Martyshov M, Emelyanov A, Demin V, Nikiruy K, Minnekhanov A, Nikolaev S, et al. Multifilamentary character of anticorrelated capacitive and resistive switching in memristive structures based on (Co- Fe- B) x (Li Nb O 3) 100-x nanocomposite. Phys Rev Appl 2020;14(3):034016.
[25] Agudov N, Safonov A, Krichigin A, Kharcheva A, Dubkov A, Valenti D, et al. Nonstationary distributions and relaxation times in a stochastic model of memristor. J Stat Mech: Theory Exp 2020;2020(2):024003.
[26] Naous R, Al-Shedivat M, Salama KN. Stochasticity modeling in memristors. IEEE Trans Nanotechnol 2015;15(1):15–28.
[27] Falci G, La Cognata A, Berritta M, D'Arrigo A, Paladino E, Spagnolo B. Design of a lambda system for population transfer in superconducting nanocircuits. Phys Rev B 2013;87(21):214515.
[28] Valenti D, Magazzù L, Caldara P, Spagnolo B. Stabilization of quantum metastable states by dissipation. Phys Rev B 2015;91(23):235412.
[29] Spagnolo B, Valenti D, Guarcello C, Carollo A, Adorno DP, Spezia S, et al. Noise-induced effects in nonlinear relaxation of condensed matter systems. Chaos Solitons Fractals 2015;81:412–24.
[30] Spagnolo B, Guarcello C, Magazzù L, Carollo A, Persano Adorno D, Valenti D. Nonlinear relaxation phenomena in metastable condensed matter systems. Entropy 2017;19(1):20.
[31] Patterson GA, Fierens PI, Grosz DF. On the beneficial role of noise in resistive switching. Appl Phys Lett 2013;103(7):074102.
[32] Mikhaylov A, Gryaznov E, Belov A, Korolev D, Sharapov A, Guseinov D, et al. Field-and irradiation-induced phenomena in memristive nanomaterials. Physica Status Solidi (c) 2016;13(10–12):870–81.
[33] Filatov D, Vrzheshch D, Tabakov O, Novikov A, Belov A, Antonov I, et al. Noise-induced resistive switching in a memristor based on ZrO2 (Y)/Ta2O5 stack. J Stat Mech: Theory Exp 2019;2019(12):124026.
[34] Erokhin V, Berzina T, Fontana M. Hybrid electronic device based on polyaniline-polyethylenoxide junction. J Appl Phys 2005;97:064501.
[35] Erokhin V, Fontana M. Thin film electrochemical memristive systems for bio-inspired computation. J Comput Theor Nanosci 2011;8:313–30.
[36] Battistoni S, Sajapin R, Erokhin V, Verna A, Cocuzza M, Marasso SL, et al. Effects of noise sourcing on organic memristive devices. Chaos, Solitons& Fractals 2020;141:110319. doi:10.1016/j.chaos.2020.110319. http://www.sciencedirect.com/science/article/pii/S0960077920307153.
[37] Berzina T, Erokhin V, Fontana MP. Spectroscopic investigation of an electrochemically controlled conducting polymer-solid electrolyte junction. J Appl Phys 2007;101(2):024501. doi:10.1063/1.2422750.
[38] Berzina T, Erokhina S, Camorani P, Konovalov O, Erokhin V, Fontana M. Electrochemical control of the conductivity in an organic memristor: A time-resolved x-ray fluorescence study of ionic drift as a function of the applied voltage. ACS Applied Materials & Interfaces 2009;1(10):2115–18. doi:10.1021/am900464k. PMID: 20355843.

[39] Demin VA, Erokhin VV, Kashkarov PK, Kovalchuk MV. Electrochemical model of the polyaniline based organic memristive device. J Appl Phys 2014;116(6):064507. doi:10.1063/1.4893022.
[40] Demin V, Erokhin V, Kashkarov P, Kovalchuk M. Electrochemical model of polyaniline-based memristor with mass transfer step. AIP Conference Proceedings 2015;1648(1):280005. doi:10.1063/1.4912534. https://aip.scitation.org/doi/abs/10.1063/1.4912534.
[41] Erokhin T, Berzina V, Camorani P, Smerieri A, Vavoulis D, Feng J, et al. Material memristive device circuits with synaptic plasticity: learning and memory. Bionanoscience 2011;1:24–30.
[42] Battistoni S, Erokhin V, Innotta S. Frequency driven organic memristive devices for neuromorphic short and long term plasticity. Org Electron 2019;65:434–8.
[43] Lapkin D, Emelyanov A, Demin V, Berzina N, Erokhin V. Spike-timing-dependent plasticity of polyaniline-based memristive element. Microelectron Eng 2018;185:43–7.
[44] Prudnikov N, Lapkin D, Emelyanov AV, Minnekhanov A, Malakhova Y, Chvalun S, et al. Associative STDP-like learning of neuromorphic circuits based on polyaniline memristive microdevices. J Phys D 2020.
[45] Talanov M, Zykov E, Erokhin V, Magid E, Distefano S, Gerasimov Y, et al. Modeling inhibitory and excitatory synapse learning in the memristive neuron model. ICINCO 2017:514–21.
[46] Talanov M, Zykov E, Erokhin V, Magid E, Distefano S. The memristive artificial neuron high level architecture for biologically inspired robotic systems. IEEE 2017:196–200.
[47] Talanov M, Zykov E, Lavrov I, Erokhin V. Bio-plausible model of electronic memristive neuron. Eur J Clin Invest 2018;48:223–4.
[48] Erokhin V, Berzina T, Camorani P, Fontana MP. On the stability of polymeric electrochemical elements for adaptive networks. Colloids and Surfaces A: Physicochemical and Engineering Aspects 2008;321(1-3):218–21. doi:10.1016/j.colsurfa.2008.02.040. https://linkinghub.elsevier.com/retrieve/pii/S0927775708001593.